

## ORIGINAL ARTICLE

# Controlled self-assembly of amphiphiles in ionic liquids and the formation of ionogels by molecular tuning of cohesive energies

Takuya Nakashima<sup>1,2</sup> and Nobuo Kimizuka<sup>1,3,4</sup>

In this paper, the self-assembling characteristics of a series of L-glutamate-based ammonium amphiphiles are studied in ionic liquids (ILs). These cationic amphiphiles are dispersible in imidazolium ILs with bis((trifluoromethyl)sulfonyl)amide (TFSA) anion. Amphiphiles-containing didodecyl ester or short dioctyl amide groups were molecularly dispersed in conventional 1-butyl-3-methylimidazolium TFSA, whereas they formed bilayer membranes when they were dispersed in polar, ether linkage-introduced IL. Thus, the modification of ILs exerts a crucial influence on amphiphilic self-assembly. Enhancement of the intermolecular interactions of L-glutamate amphiphiles is achieved by introducing multiple amide bonds and longer alkyl chains, which leads to better self-assembling properties. These amide-enriched amphiphiles form fibrous bilayer assemblies even in conventional ILs with low cohesive energy densities. These observations confirm that the formation of bilayer membranes in ILs is a general phenomenon when the solute molecules have the appropriate ‘ionophilic/ionophobic’ nature.

*Polymer Journal* (2012) 44, 665–671; doi:10.1038/pj.2012.73; published online 25 April 2012

**Keywords:** amphiphile; bilayer membrane; ionic liquid; ionogel; self-assembly

## INTRODUCTION

Room temperature ionic liquids (ILs) are attracting significant interest as environmentally benign solvents for organic chemical reactions,<sup>1</sup> separations<sup>2</sup> and electrochemical applications<sup>3,4</sup> because of their unique properties including their very low vapor pressure, high ionic conductivity and limited miscibility with water and common organic solvents.<sup>5</sup> Some recent studies also highlighted their use in inorganic synthesis,<sup>6–9</sup> hybridization with nanocarbons<sup>10,11</sup> and molecular self-assembly.<sup>12–15</sup> One of the advantageous features of ILs for their application in supramolecular chemistry is expressed in terms of solvent engineering, that is, the properties of ILs can be readily tuned based on their molecular structures. Traditionally, the structures and properties of amphiphilic molecular self-assembling systems have been tuned by designing the constituent molecules.<sup>16,17</sup> Yet, cohesive interactions between the constituent amphiphilic molecules, their dispersibility (stabilization of the interface between amphiphilic self-assemblies and solvents) and the interactions among solvent molecules all contribute to self-assembly. For example, bilayer membranes are formed not only in water but also in organic solvents including protic and aprotic organic solvents.<sup>16,18,19</sup> The double-chained fluorocarbon amphiphiles with solvophilic hydrocarbon chains form bilayer membranes in aprotic organic solvents.<sup>20</sup>

The simultaneous pursuit of ‘amphiphilicity’ and ‘intermolecular interactions’ has been further manifested by the complementary hydrogen bond networks in organic<sup>21</sup> and aqueous media.<sup>22</sup>

The use of ILs as solvents further enables the systematic study of molecular design to achieve amphiphilic self-assembly in ionic media. The desired molecules should consist of solvophilic (ionophilic) and solvophobic (ionophobic) groups, as we have shown previously in the first example of synthetic bilayer membranes formed in ether-containing ILs.<sup>23,24</sup> Ether-containing ILs that carry a bromide counter anion showed sugarphilic properties, that is, an excellent ability to dissolve carbohydrates including glucose, cyclodextrin, amylose and glycosylated proteins.<sup>23</sup> This finding was successfully applied to dissolve cellulose.<sup>25</sup> A synthetic glycolipid developed fibrous nanostructures in the ether-containing ILs, representing the first example of physically gelatinized ILs by self-assembly (ionogels).<sup>23</sup> The bilayer self-assemblies in ILs show different characteristics compared with those formed in water, as demonstrated for *N,N*-dialkylammonium bromides.<sup>24</sup> Experimentation showed that *N,N*-dialkylammonium bromides formed vesicles in the ether-containing ILs, indicating that the ammonium head groups served as an ionophilic moiety and that the alkyl chains exerted ionophobic properties.<sup>24</sup> Interestingly, the gel-to-liquid-crystalline phase transition

<sup>1</sup>Department of Chemistry and Biochemistry, Graduate School of Engineering, Kyushu University, Fukuoka, Japan; <sup>2</sup>Graduate School of Materials Science, Nara Institute of Science and Technology, Nara, Japan; <sup>3</sup>Center for Molecular Systems (CMS), Kyushu University, Fukuoka, Japan and <sup>4</sup>Japan Science and Technology Agency (JST), CREST, Japan

Correspondence: Professor N Kimizuka, Department of Chemistry and Biochemistry, Graduate School of Engineering, Kyushu University, 744 Moto-oka Nishi-ku, Fukuoka 819-0395, Japan.

E-mail: n-kimi@mail.cstm.kyushu-u.ac.jp

Received 31 December 2011; revised 21 March 2012; accepted 22 March 2012; published online 25 April 2012

temperatures ( $T_c$ ) observed in these ILs were significantly elevated compared with those observed for aqueous bilayers.<sup>26</sup> This effect is ascribed to the enhanced intermolecular cohesive forces resulting from the shielding of electrostatic repulsion operating between the ammonium head groups.<sup>24</sup> Thus, self-assembly in ILs exhibits unique features not available in the aqueous or common organic solvent systems. The abovementioned works led to the subsequent formation of supramolecular ionogels from low-molecular-weight gelators,<sup>27–30</sup> oligomeric electrolytes<sup>31</sup> and nano-assemblies by metal-fluorous surfactant complexes,<sup>32</sup> amphiphilic polymers<sup>33</sup> and block-copolymers.<sup>34</sup>

To elucidate amphiphilic self-assembly phenomena in a wide range of ILs and to systematize this behavior, it is necessary to understand correlative relationships between the properties of the self-assemblies and the chemical structures of solute amphiphiles in ILs with varying cohesive energy densities. It should also be noted that ILs can be amphiphilic<sup>35</sup> and capable of forming ionic hydrogen bonds.<sup>36</sup> We describe herein the formation of bilayer membranes in ILs for a series of aqueous-bilayer-forming cationic glutamate amphiphiles. The intermolecular interactions required for self-assembly in ILs vary depending on the chemical structure of ILs, and these results provide a general guideline to design ordered molecular self-assembly systems in ILs.

## EXPERIMENTAL PROCEDURE

### General

The water content of ILs was determined by the Karl Fischer's method using a CA-07 Moisturemeter (Mitsubishi Chemical Analytech. Co. Ltd Kanagawa, Japan) and found to be 0.08 wt% for  $C_1OC_1mimTFSA$  (bis((trifluoromethyl)sulfonyl)amide) and 0.07 wt% for 1-butyl-3-methylimidazolium TFSA ( $C_4mimTFSA$ ). The amphiphiles were dispersed in ILs with ultrasonication by a Branson Sonifier Model 185 (Branson, Danbury, CT, USA; sonic power 40 W, 1–2 min). Dark-field optical measurements were carried out by an Olympus BHF (Olympus Corp., Tokyo, Japan). Fourier transform infrared (FT-IR) spectra were recorded on a Nicolet 820 FT-IR spectrometer (Thermo Nicolet Inc., Madison, WI, USA). The solution or ionogel samples were sandwiched between two BaF<sub>2</sub> plates with a 0.1-mm Teflon spacer. Differential scanning calorimetry (DSC) was measured by a Seiko SSC5200 calorimeter (Seiko Instruments Inc., Chiba, Japan).

### Synthesis

ILs were synthesized according to the literature<sup>37</sup> and confirmed by <sup>1</sup>H nuclear magnetic resonance (H NMR) and elemental analysis. Amphiphiles 1–4 were prepared<sup>38,39</sup> and identified by FT-IR, NMR spectra and by elemental analyses.

### 1-Methoxymethyl-3-methylimidazolium TFSA, $C_1OC_1mimTFSA$

LiTFSI (20 g, 70 mmol) was added to an aqueous solution of  $C_1OC_1mimBr$  (12 g, 58 mmol), and the mixture was stirred for 5 h. The mixture was phase separated, and the bottom layer was collected, repeatedly washed with deionized water and dried *in vacuo* at 60 °C to give 14 g (35 mmol) of  $C_1OC_1mimTFSA$  at 60% yield. <sup>1</sup>H NMR (250 MHz, acetone-*d*<sub>6</sub>, tetramethylsilane (TMS)):  $\delta$  9.08 (s, 1H), 7.90 (d, 1H), 7.82 (d, 1H), 5.70 (s, 2H), 4.14 (s, 3H), and 3.46 (s, 3H). Anal. calcd. for C<sub>8</sub>H<sub>11</sub>F<sub>6</sub>N<sub>3</sub>O<sub>5</sub>S<sub>2</sub>: C, 23.59; H, 2.83; and N, 10.32. The found values were as follows: C, 23.57; H, 2.72; and N, 10.33.

### 1-Butyl-3-methylimidazolium TFSA

This compound was prepared by the same procedure as was used for  $C_1OC_1mimTFSA$ , except that  $C_1OC_1mimBr$  was replaced by  $C_4mimBr$ . From 12 g (55 mmol) of  $C_4mimBr$  and 16 g (57 mmol) LiTFSI,  $C_4mimTFSA$  (19 g, 45 mmol) was obtained at 82% yield. <sup>1</sup>H NMR (250 MHz, methanol-*d*<sub>4</sub>, TMS):  $\delta$  9.17 (s, 1H), 7.52 (d, 1H), 7.45 (d, 1H), 4.11 (t, 2H), 3.83 (s, 3H), 1.78 (m, 2H), 1.28 (m, 2H), and 0.95 (t, 3H). Anal. calcd. for C<sub>10</sub>H<sub>15</sub>F<sub>6</sub>N<sub>3</sub>O<sub>4</sub>S<sub>2</sub>: C,

28.64; H, 3.61; and N, 10.02. The found values were as follows: C, 28.48; H, 3.66; and N, 10.18.

### *N*-(11-(2-hydroxyethyl)dimethylammonium)undecanoyl-*O*,*O'*-didodecyl-L-glutamate bromide, 1

FT-IR (KBr)  $\nu$ (O–H) 3400 cm<sup>-1</sup>,  $\nu$ (N–H) 3335 cm<sup>-1</sup>,  $\nu$ (C–H) 2920, 2849 cm<sup>-1</sup>,  $\nu$ (C=O) 1732, 1654 cm<sup>-1</sup> and  $\delta$ (N–H) 1526 cm<sup>-1</sup>. <sup>1</sup>H NMR(250 MHz, CDCl<sub>3</sub>, TMS):  $\delta$  6.37 (d, 1H), 4.59 (q, 1H), 4.14 (b, 2H), 4.12, 4.05 (t + t, 2H + 2H), 3.68 (t, 2H), 3.53 (t, 2H), 3.37 (s, 6H), 2.42, 2.32 (m, 2H), 2.23 (t, 2H), 2.18, 2.00 (m, 1H + 1H), 1.76 (m, 2H), 1.63 (m, 6H), 1.2–1.5 (m, 48H), 0.88 (t, 6H). Anal. calcd. for C<sub>36</sub>H<sub>73</sub>O<sub>4</sub>N<sub>4</sub>Br: C, 64.44; H, 10.69; and N, 3.42. The found values were as follows: C, 64.59; H, 10.67; and N, 3.46.

### *N*-(11-(2-hydroxyethyl)dimethylammonium)undecanoyl)-*N*,*N'*-dioctyl-L-glutamate bromide, 2<sup>38</sup>

FT-IR (KBr)  $\nu$ (O–H) 3400 cm<sup>-1</sup>,  $\nu$ (N–H) 3293 cm<sup>-1</sup>,  $\nu$ (C–H) 2924, 2853 cm<sup>-1</sup>,  $\nu$ (C=O) 1639 cm<sup>-1</sup> and  $\delta$ (N–H) 1561 cm<sup>-1</sup>. <sup>1</sup>H NMR(250 MHz, CDCl<sub>3</sub>, TMS):  $\delta$  7.57 (d, 1H), 7.37 (t, 1H), 6.88 (t, 1H), 4.39 (m, 1H), 4.11 (t, 2H), 3.72 (t, 2H), 3.58 (t, 2H), 3.36 (s, 6H), 3.17 (m, 4H), 2.30 (m, 2H), 2.23 (t, 2H), 2.05 (m, 2H), 1.78 (m, 2H), 1.5–1.8 (m, 6H), 1.2–1.5 (m, 32H), 0.87 (t, 6H). Anal. calcd. for C<sub>36</sub>H<sub>73</sub>O<sub>4</sub>N<sub>4</sub>Br: C, 61.25; H, 10.42; and N, 7.94. The found values were as follows: C, 61.73; H, 10.40; and N, 8.03.

### *N*-(11-(2-hydroxyethyl)dimethylammonium)undecanoyl)-*N*,*N'*-didodecyl-L-glutamate bromide, 3<sup>39</sup>

FT-IR (KBr)  $\nu$ (O–H) 3400 cm<sup>-1</sup>,  $\nu$ (N–H) 3293 cm<sup>-1</sup>,  $\nu$ (C–H) 2923, 2853 cm<sup>-1</sup>,  $\nu$ (C=O) 1638 cm<sup>-1</sup> and  $\delta$ (N–H) 1561 cm<sup>-1</sup>. <sup>1</sup>H NMR (250 MHz, CDCl<sub>3</sub>, TMS):  $\delta$  7.5 (d, 1H), 6.6 (t, 1H), 5.2 (t, 1H), 4.4 (m, 1H), 4.2 (t, 2H), 3.79 (t, 2H), 3.6 (t, 2H), 3.4 (s, 6H), 3.2 (m, 4H), 2.3 (m, 2H), 2.2 (t, 2H), 2.0 (m, 2H), 1.8 (m, 2H), 1.6 (m, 2H), 1.4–1.5 (m, 4H), 1.2–1.4 (m, 48H), 0.9 (t, 6H). Anal. calcd. for C<sub>44</sub>H<sub>89</sub>O<sub>4</sub>N<sub>4</sub>Br: C, 64.60; H, 10.97; and N, 6.85. The found values were as follows: C, 64.30; H, 10.97; and N, 6.66.

### *N*-(11-(2-hydroxyethyl)dimethylammonium)undecanoyl)-*N*,*N'*-di(3-dodecyloxypropyl)-L-glutamate bromide, 4

FT-IR (KBr)  $\nu$ (O–H) 3400 cm<sup>-1</sup>,  $\nu$ (N–H) 3300 cm<sup>-1</sup>,  $\nu$ (C–H) 2920, 2850 cm<sup>-1</sup>,  $\nu$ (C=O) 1640 cm<sup>-1</sup> and  $\delta$ (N–H) 1560 cm<sup>-1</sup>  $\nu$ (C–O–C) 1120 cm<sup>-1</sup>; <sup>1</sup>H NMR (250 MHz, CDCl<sub>3</sub>, TMS):  $\delta$  7.5 (d, 1H), 7.3 (t, 1H), 6.9 (t, 1H), 4.4 (m, 1H), 4.2 (t, 2H), 3.8 (t, 2H), 3.3–3.7 (m, 20H), 2.2–2.4 (m, 4H), 1.7–2.1 (m, 12H), 1.4–1.6 (m, 4H), 1.2–1.4 (m, 48H), 0.9 (t, 6H). Anal. calcd. for C<sub>50</sub>H<sub>101</sub>O<sub>6</sub>N<sub>4</sub>Br: C, 64.28; H, 10.90; and N, 6.00. The found values were as follows: C, 64.36; H, 10.83; and N, 5.98.

## RESULTS AND DISCUSSION

Cationic amphiphiles 1–4 depicted in Figure 1 all possess glutamate-based structures, which are known to promote the formation of stable bilayer membranes in water.<sup>16,38,39</sup> Table 1 summarizes their morphology and gel-to-liquid-crystalline phase transition behaviors in aqueous bilayers. Amphiphile 1 formed vesicles in water, with a gel-to-liquid-crystalline phase transition temperature  $T_c$  of 33 °C. On the other hand, amphiphiles 2 and 3 showed higher  $T_c$  (69 °C for 2, 87 °C for 3), indicating that the introduction of amide linkages and longer alkyl chains strengthens intermolecular interactions and consequently enhances the thermal stability of the gel phase.<sup>16,38</sup>

### Dispersion behavior of amphiphiles 1–4 in ILs

Amphiphiles 1–4 were dispersed in ILs ( $C_1OC_1mimTFSA$  and  $C_4mimTFSA$ , Figure 1) by ultrasonication for a few minutes at room temperature. Table 2 summarizes the appearance of 1–4 (10 mM) in ILs and reports the dissolution temperatures of the ionogels  $T_{GS}$ . The term ionogel indicates physically gelatinized ILs formed by polymers or low-molecular-weight gelator molecules, similar to the terms

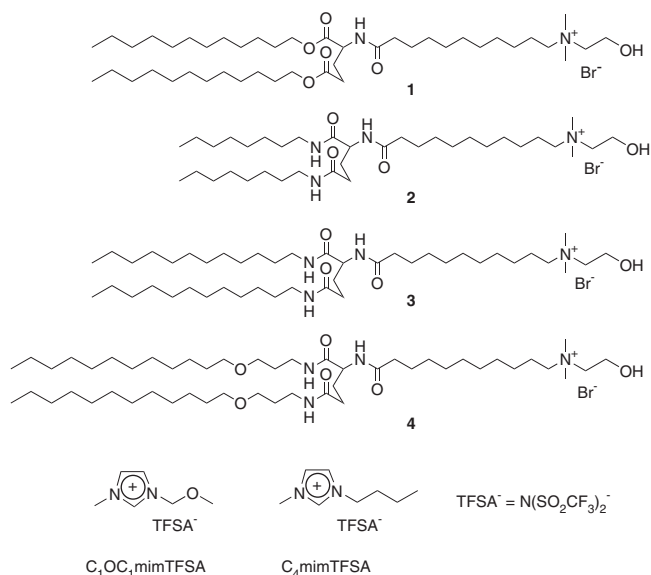


**Figure 1** Molecular structures of cationic glutamate amphiphiles **1–4** and ILs.

**Table 1** Self-assembling properties of amphiphiles **1–4** in water

Amphiphile	Morphology	Thermodynamic parameters <sup>a</sup>		
		$T_c$ (°C)	$\Delta H$ (kJ mol <sup>-1</sup> )	$\Delta S$ (J mol <sup>-1</sup> K <sup>-1</sup> )
<b>1</b>	Vesicle	33.0	50.3	164.4
<b>2<sup>b</sup></b>	Fiber	69.0	11.3	33.2
<b>3<sup>c</sup></b>	Fiber	87.0	26.0	72.3
<b>4</b>	Helical ribbon	46.6, 51.7	48.9	148.0

<sup>a</sup>Based on gel-to-liquid-crystal phase transition in water.

<sup>b</sup>Reference Nakashima *et al.*<sup>38</sup>

<sup>c</sup>Reference Kimizuka *et al.*<sup>39</sup>

**Table 2** Appearance of dispersions in ILs and their gel–sol transition temperatures ( $T_{GS}$ )<sup>a</sup>

Amphiphile	$C_1OC_1mimTfSA$	$C_4mimTfSA$
<b>1</b>	S (translucent)	S (clear)
<b>2</b>	IG (transparent) $T_{GS} = 45$ °C	S (clear)
<b>3</b>	IG (opaque) $T_{GS} = 68$ °C	IG (opaque) $T_{GS} = 61$ °C
<b>4</b>	IG (opaque) $T_{GS} = 46$ °C	IG (opaque) $T_{GS} = 50$ °C

Abbreviations: IG, ionogel formed at room temperature; IL, ionic liquids; S, solution; TfSA, bis((trifluoromethyl)sulfonyl)amide;  $T_{GS}$ , the temperature gel flows as determined visually.

<sup>a</sup>Concentration of amphiphiles: 10 mM.

‘hydrogel’ or ‘organogel,’ with the names indicating the solvents that are gelatinized.<sup>23</sup> Each amphiphile produced a stable dispersion in the used ILs without precipitation. Amphiphile **2**, having shorter octyl chains with amide linkages, formed a transparent ionogel in the ether-containing  $C_1OC_1mimTfSA$ , whereas it dissolved as a clear solution in  $C_4mimTfSA$ . Conversely, increasing the chain length (**2–3**) markedly enhanced self-assembly, and opaque ionogels were obtained for both of the abovementioned ILs.

#### Self-assembly of amphiphiles **1** and **2**

Amphiphile **1** formed translucent and clear dispersions in  $C_1OC_1mimTfSA$  and  $C_4mimTfSA$ , respectively. These visual

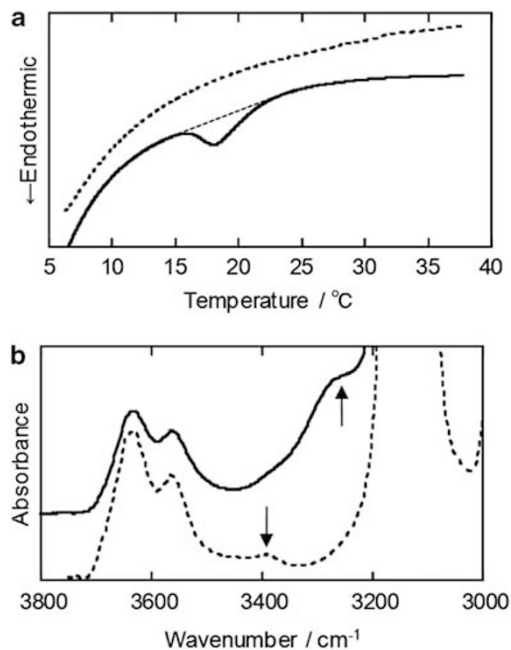


**Figure 2** (a) DCS thermograms and (b) FT-IR spectra of the N–H and O–H regions of amphiphile **1** in  $C_1OC_1mimTfSA$  (solid line) and  $C_4mimTfSA$  (broken line), (**1**) = 10 mM.

characteristics were reflected in the DSC thermograms and FT-IR spectra. Figure 2a shows DSC thermograms of **1** dispersed in  $C_1OC_1mimTfSA$  and  $C_4mimTfSA$ . In  $C_1OC_1mimTfSA$ , **1** showed an endothermic peak  $T_c$  at 17.9 °C (solid line,  $\Delta H$ , 18.0 kJ mol<sup>-1</sup>,  $\Delta S$ , 61.8 JK<sup>-1</sup> mol<sup>-1</sup>), which is ascribed to a gel-to-liquid-crystalline phase transition typically observed for bilayer membranes. In contrast, **1** gave no apparent DSC peaks in  $C_4mimTfSA$  (dashed line). In FT-IR, a stretching vibration of amide N–H appeared at 3280 cm<sup>-1</sup> in  $C_1OC_1mimTfSA$  as a shoulder, whereas it was observed at 3393 cm<sup>-1</sup> in  $C_4mimTfSA$  (Figure 2b). The low frequency shift (by  $\sim 113$  cm<sup>-1</sup>) observed for **1** in  $C_1OC_1mimTfSA$  can be explained by the formation of intermolecular hydrogen bonds between amphiphile **1**, indicating self-assembly in the ether linkage-introduced IL.

The formation of ordered self-assemblies was also supported by dark-field optical microscopy (Figure 3). When amphiphile **1** was dispersed in  $C_1OC_1mimTfSA$ , vesicular structures with diameters of 3–10  $\mu$ m were observed at room temperature. In contrast, no aggregate structure was observed in  $C_4mimTfSA$ . Apparently, amphiphile **1** formed bilayer membranes in  $C_1OC_1mimTfSA$ , whereas it was molecularly dispersed in  $C_4mimTfSA$ . The size of the observed vesicles in  $C_1OC_1mimTfSA$  was also considerably larger than those observed in aqueous dispersions (diameters  $\sim 150$ –400 nm). As the curvature of lipid vesicles has been related to the cross-sectional area of solvated lipid head groups, the decreased curvature of vesicles in  $C_1OC_1mimTfSA$  reflects the enhanced packing density of cationic head groups. This would be caused by the shielding of electrostatic repulsion between the ammonium head groups of amphiphile **1** aligned on the vesicle surface.<sup>24</sup>

The effect of the IL molecular structure is also prominent for the short-legged amphiphile **2**. When **2** was dissolved in  $C_4mimTfSA$ , a clear homogeneous solution was obtained, as described previously. The N–H stretching band of **2** in  $C_4mimTfSA$  was observed at 3398 cm<sup>-1</sup> (Figure 4b, broken line), indicating that **2** was molecularly

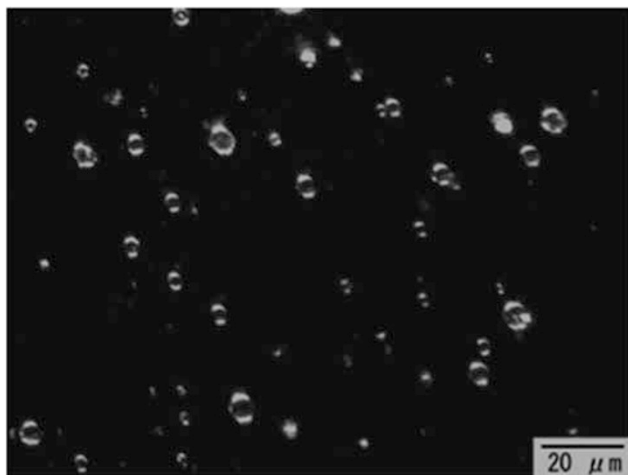


**Figure 3** Dark-field optical micrograph of amphiphile **1** in  $C_1OC_1mimTFSA$ , (**1**) = 10 mM.

dispersed without forming intermolecular hydrogen bonds. In contrast, **2** surprisingly formed fibrous superstructures as observed by dark-field optical microscopy and consequently formed ionogels in ether-containing  $C_1OC_1mimTFSA$  (10 mM, Figure 4a). The ionogel formed from **2** in  $C_1OC_1mimTFSA$  exhibited a stretching vibrational N–H peak at  $3285\text{ cm}^{-1}$ , and the observed shorter wavenumber shift is consistent with the formation of hydrogen bond networks in ordered bilayer assemblies.

We have previously reported that amphiphile **2** alone in water gives a viscous dispersion of the bilayer membrane, which becomes gelatinized upon the addition of hydrophobic aromatic anions.<sup>38</sup> The hydrophobic anions effectively shielded the electrostatic repulsion between nanofibers and promoted their contacts, resulting in the formation of hydrogels. In this case, the electrostatic repulsion between charged fibrous nanostructures in ILs should also be effectively screened by the adsorption of TFSA ions, resulting in the observed physical gelation of ILs. It is noteworthy that the electrostatic binding of the TFSA anion to **1** and **2** enhances the solubility of these amphiphiles in ILs, as they were not able to be dispersed in imidazolium salts with bromide anions ( $C_1OC_1mimBr$  and  $C_4mimBr$ ), even at elevated temperatures ( $>100\text{ }^\circ\text{C}$ ).

Imidazolium-based ILs are reported to form ionic hydrogen bonds of the form  $C(2)-H\cdots A^-$  (A, anion), and bonds formed between 1-ethyl-3-methyl-imidazolium and TFSA anion were reported by Fumino *et al.*<sup>36</sup> Meanwhile, ILs with TFSA anions were reported to possess a significantly smaller cohesive energy density than water.<sup>13</sup> The observation that **1** and **2** are molecularly dispersed in  $C_4mimTFSA$  without forming self-assemblies can be understood by the insufficient difference in cohesive energy between **1**, **2** and  $C_4mimTFSA$ .<sup>23,24</sup> The difference in cohesive energy between solutes and solvents is an essential feature required for self-assembly in a given media.<sup>20</sup>

In contrast, **1** and **2** form developed bilayer membranes in  $C_1OC_1mimTFSA$ , which clearly indicates the excellent performance of  $C_1OC_1mim$  ions as a solvent for molecular assemblies. Ether groups possess a higher electron density because of the lone pairs located on the oxygen atom, which are known to show an affinity to cations (ionophilic nature). Accordingly, introduction of the ether linkage to  $C_1OC_1mim$  not only enhances the polarity of the IL but also gives it a better ability to solvate ammonium bilayers.<sup>24</sup> It is also possible that the ether linkage in  $C_1OC_1mim$  interacts with the C(2)–

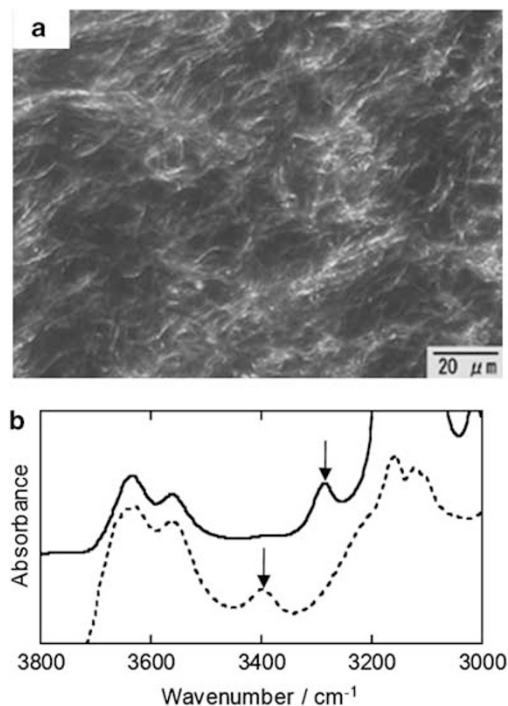


**Figure 4** (a) Dark-field optical micrograph of ionogel **2** in  $C_1OC_1mimTFSA$ . (b) FT-IR spectra of the N–H and O–H regions of **2** in  $C_1OC_1mimTFSA$  (solid line) and  $C_4mimTFSA$  (broken line), (**2**) = 10 mM.

H proton of the imidazolium ring by hydrogen bonding.<sup>40</sup> These features lead to sufficient differences in cohesive energy between ammonium amphiphiles and  $C_1OC_1mimTFSA$ , providing immiscibilities between them and allowing ammonium bilayer membranes to be stably dispersed.

#### Self-assembly of amphiphiles **3** and **4**

The glutamate amphiphiles **3** and **4** possess multiple amide linkages and long alkyl chains, which impart enhanced cohesive energies and accordingly lead to more self-assembly by these amphiphiles. This is clearly shown by the observed formation of self-assembling ionogels in both of the ILs,  $C_1OC_1mimTFSA$  and  $C_4mimTFSA$ . Developed fibrous assemblies were observed for all the ionogels of **3** and **4** by dark-field optical microscopy (Figure 5a, Supplementary Figures S2 and 3 in the Supplementary Information). The formation of developed hydrogen bond networks in these ILs were confirmed by FT-IR spectroscopy (Table 3), which contain vibrational N–H peaks at shorter wave numbers of  $3279\text{ cm}^{-1}$  (**3** in  $C_1OC_1mimTFSA$ ),  $3283\text{ cm}^{-1}$  (**3** in  $C_4mimTFSA$ ),  $3276\text{ cm}^{-1}$  (**4** in  $C_1OC_1mimTFSA$ ) and  $3280\text{ cm}^{-1}$  (**4** in  $C_4mimTFSA$ ). These ionogels also gave gel-to-liquid-crystalline phase transition peaks in DSC (Table 3, Supplementary Figure S1 in the Supplementary Information), indicating that **3** and **4** form bilayer membrane-based developed structures in these ILs. Note that the gel-to-liquid-crystalline phase transition temperatures  $T_c$  observed for **3** and **4** in  $C_1OC_1mimTFSA$  (**3**:  $72.3\text{ }^\circ\text{C}$ , **4**:  $56.9\text{ }^\circ\text{C}$ ) are significantly higher than those observed in  $C_4mimTFSA$  (**3**:  $64.7\text{ }^\circ\text{C}$ , **4**:  $46.8\text{ }^\circ\text{C}$ ). Thermodynamic parameters ( $\Delta H$ ,  $\Delta S$ ) also show the same trend, with larger values observed in  $C_1OC_1mimTFSA$  compared with  $C_4mimTFSA$ . These observations clearly indicate that the thermal stability of the gel-phase lipid bilayers **3** and **4** is much higher in  $C_1OC_1mimTFSA$ . It is apparent that  $C_1OC_1mimTFSA$  stably disperses bilayers without deteriorating their

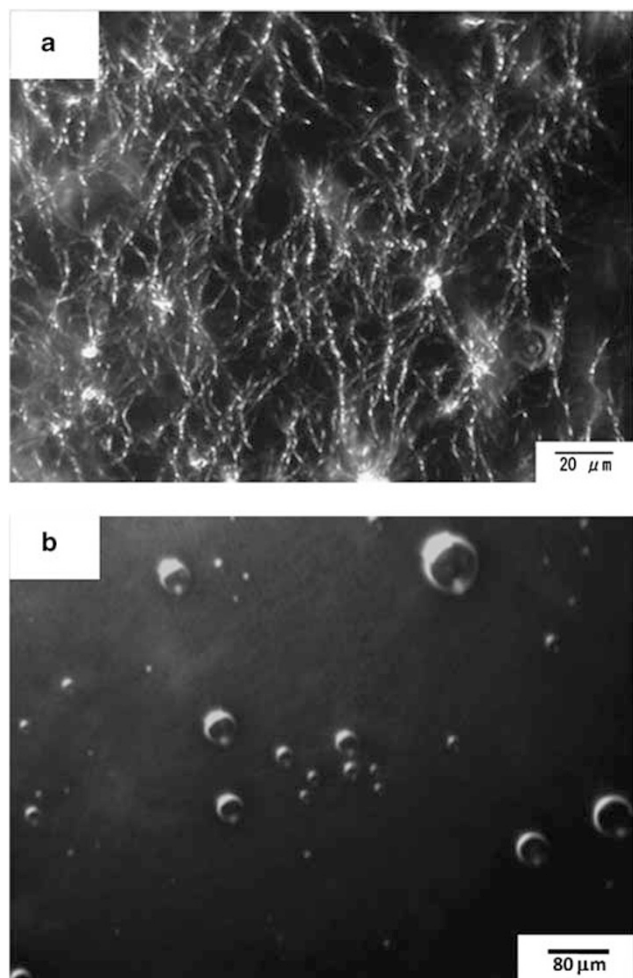


**Figure 5** Dark-field optical micrographs of amphiphile **4** in  $C_1OC_1mimTFSA$  (a). At room temperature (ionogel) and (b) above  $T_c$  (60 °C).

**Table 3** FT-IR (amide strfatching) and DSC data for amphiphiles **3** and **4**<sup>a</sup>

Amphiphile		$C_1OC_1mimTFSA$	$C_4mimTFSA$
<b>3</b>	$\nu(N-H)$	3279	3283
	$\nu(C=O)$	1633	1633
	$T_c$ (°C)	72.3	64.7
$(\Delta H$ (kJmol <sup>-1</sup> ), $\Delta S$ (JK <sup>-1</sup> mol <sup>-1</sup> ))		(13.3, 38.6)	(4.37, 12.9)
<b>4</b>	$\nu(N-H)$	3276	3280
	$\nu(C=O)$	1633	1635
	$T_c$ (°C)	56.9	46.8
$(\Delta H$ (kJmol <sup>-1</sup> ), $\Delta S$ (JK <sup>-1</sup> mol <sup>-1</sup> ))		(15.7, 47.5)	(3.17, 9.90)

Abbreviations: DSC, differential scanning calorimetry; FT-IR, Fourier transform infrared; TFSA, bis((trifluoromethyl)sulfonyl)amide.

<sup>a</sup>Concentration of amphiphiles: 10 mM

regular molecular alignment, and therefore it does not penetrate as far into the packed alkyl chain region. In contrast, hydrophobic  $C_4mimTFSA$  molecules penetrate into the bilayer interior, which inevitably disturbs the molecular alignment of bilayers. Thus, the thermodynamic properties of bilayers dispersed in ILs are strongly affected by the molecular structures of both constituents. It should be

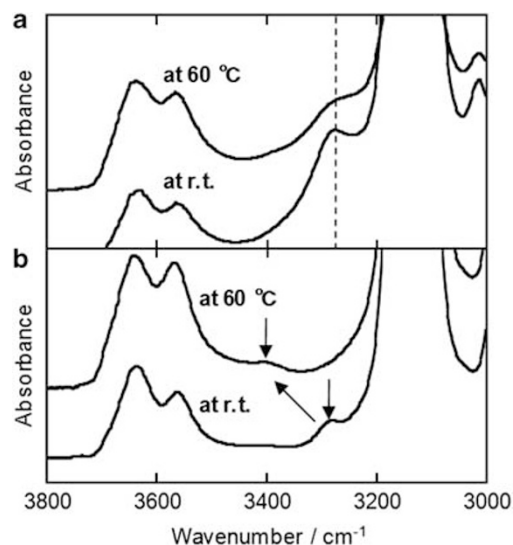


**Figure 6** The temperature dependence of FT-IR spectra. Amide N-H stretching vibrational peaks of **4** in (a)  $C_1OC_1mimTFSA$  and in (b)  $C_4mimTFSA$ .

emphasized that enhancing the cohesive energy of amphiphiles by introducing multiple amide bonds or longer alkyl chains is crucial to maintain sufficient intermolecular interactions to form ordered bilayer membranes and ionogels, even in conventional ILs such as  $C_4mimTFSA$ .

Next, the thermal properties of the ionogels were investigated in more detail. Upon heating, ionogels formed from **3** and **4** above the temperature of  $T_{GS}$  became liquefied.  $T_{GS}$  did not necessarily correspond to the gel-to-liquid-crystalline phase transition temperature  $T_c$ . Interestingly, upon heating the ionogel of ether-containing amphiphile **4** in  $C_1OC_1mimTFSA$  to the liquid-crystalline phase transition temperature  $T_c$ , a morphological transformation from nanofibers to vesicles was observed (Figure 5). Developed nanofibrous structures fused into large vesicles upon heating, whereas these vesicles underwent a reversible transformation into fibers upon cooling to room temperature. A similar nanofiber-to-vesicle transformation was also observed for ionogels formed from ether-containing glycolipid bilayer membranes.<sup>23</sup> However, fibrous structures observed for the other ionogels (**3** in  $C_1OC_1mimTFSA$  and  $C_4mimTFSA$ , **4** in  $C_4mimTFSA$ ) disappeared upon heating above the gel-to-liquid-crystalline temperatures.

Figure 6 compares thermally induced FT-IR spectral changes observed for ionogels **4** formed in  $C_1OC_1mimTFSA$  (a) and  $C_4mimTFSA$  (b). Upon heating the  $C_1OC_1mimTFSA$  ionogel above  $T_c$  (60 °C), the  $\nu(N-H)$  peak position of **4** was kept unchanged (Figure 6a). This result clearly indicates that the intermolecular hydrogen bonds formed between amide linkages were even maintained in vesicles. In contrast, the  $\nu(N-H)$  peak position of ionogel **4** in  $C_4mimTFSA$  at 3280 cm<sup>-1</sup> markedly shifted to 3400 cm<sup>-1</sup> upon heating (Figure 6b). This result indicates that hydrogen bonding is destroyed above the gel-to-liquid-crystalline temperature. Together with the observed disappearance of aggregate structures in dark-field optical microscopy, these results demonstrate that the amphiphile **4** is molecularly dispersed in  $C_4mimTFSA$  by heating above the  $T_c$ .

It is interesting that thermally stable bilayer membranes that display structural transformations from nanofibers to vesicles can be obtained by introducing multiple amide bonds and ether linkages into the lipid

**Table 4** Features for amphiphilic self-assembly in varied media—water, organic solvents and ionic liquids (ILs)

Solvents		Water	Organic solvents	ILs
Cohesive energy density of solvents		High	Low	Tailorable by molecular design, for example, anions, introduction of the ether linkage, and so on.
Molecular interactions	Van der Waals	Yes	Yes	Yes
	Electrostatic	Yes	Yes	Weak (shielded)
	H bonding	Weak <sup>a</sup>	Yes	Yes
Amphiphilic design		Hydrophilic/hydrophobic	Solvophilic/solvophobic	Ionophilic/ionophobic
Gels formed by self-assembly		Yes: hydrogels	Yes: organogels	Yes: ionogels

<sup>a</sup>Water molecules compete with the formation of hydrogen bonds.

chemical structure. This structural feature is common to the ionogel-forming glycolipid.<sup>23</sup> Apparently, the introduction of ether linkages in the alkyl chain of amphiphiles serves to enhance the integrity of bilayers in ILs. We previously reported that introducing flexible ether linkages into amphiphilic structures improved the molecular ordering in bilayer membranes<sup>41</sup> and supramolecular membranes<sup>22</sup> in water. These observations account for the role of flexible ether linkages that improve the molecular alignment of alkyl chains by allowing them to regularly pack even in the presence of molecular orientational demands required by the other structural modules such as glutamate connectors and ammonium head groups. The stabilization of vesicle structures occurred uniquely to the ether-containing amphiphile **4** in  $C_1OC_1mimTFSA$ , and this stabilization may involve the contribution of other cohesive interactions such as dipole–dipole interactions among aligned alkyl ether groups in the liquid crystalline state. Therefore, molecular self-assembly in designed ILs provides an opportunity to learn more about the contribution of intermolecular interactions exerted by constituent molecular units. This information provides important guidelines for the design of regularly oriented molecular assemblies in ILs, which lay the foundation for soft nanomaterial chemistry.

## CONCLUSION

In conclusion, stable bilayer membranes and ionogels were developed from a series of L-glutamate-based ammonium amphiphiles. The formation of bilayer membranes in ILs is a general phenomenon that occurs even for ILs with low cohesive energies. Table 4 summarizes the features of self-assembly in three solvent systems. The high cohesive energy of water leads to the hydrophobic self-assembly of amphiphilic molecules. Water molecules compete for hydrogen bonds among the solutes, and this formation of hydrogen bonds in aqueous media requires hydrophobic components to be kept away from the bulk water.<sup>16,22</sup> In organic solvents, the cohesive energy density of the media is generally small and the self-assembly of ordered molecular assemblies requires both amphiphilic (solvophilic/solvophobic) molecular design and increased cohesive energies between the solute molecules.<sup>16,20,21</sup> These points are essentially the same for self-assembly in ILs. The unique feature of ILs that is not available in other solvents is that electrostatic repulsions are shielded as expected based on the nature of the ionic media. It should be emphasized that differences in the cohesive energies of ILs and solute molecules are important to direct self-assembly in ILs and control their properties. The polarity and cohesive energy of ILs are easily tunable, as clearly shown by the introduction of ether linkages in ILs. The introduction of hydrogen bonds, longer alkyl chains and ether linkages effectively enhanced the cohesive interactions of the solute amphiphilic

molecules. Molecular self-assemblies formed in ILs display unique properties and functionalities that are not available in aqueous or conventional organic media, and we envisage a wide range of functional applications of these new soft nanomaterials.

## ACKNOWLEDGEMENTS

This work is in part supported by the JST CREST. The authors are grateful to Professor M Goto (Kyushu University) for the use of the CA-07 Moisturemeter.

- 1 Parvulescu, V. I. & Hardacre, C. Catalysis in ionic liquids. *Chem. Rev.* **107**, 2615–2665 (2007).
- 2 Han, X. & Armstrong, D. W. Ionic liquids in separations. *Accounts Chem. Res.* **40**, 1079–1086 (2007).
- 3 MacFarlane, D. R., Pringle, J. M., Howlett, P. C. & Forsyth, M. Ionic liquids and reactions at the electrochemical interface. *Phys. Chem. Chem. Phys.* **12**, 1659–1669 (2010).
- 4 Armand, M., Endres, F., MacFarlane, D. R., Ohno, H. & Scrosati, B. Ionic-liquid materials for the electrochemical challenges of the future. *Nat. Mater.* **8**, 621–629 (2009).
- 5 Seddon, K. R., Stark, A. & Torres, M. J. Influence of chloride, water, and organic solvents on the physical properties of ionic liquids. *Pure Appl. Chem.* **72**, 2275–2287 (2000).
- 6 Nakashima, T. & Kimizuka, N. Interfacial synthesis of hollow TiO<sub>2</sub> microspheres in ionic liquids. *J. Am. Chem. Soc.* **125**, 6386–6387 (2003).
- 7 Antonietti, M., Kuang, D. B., Smarsly, B. & Yong, Z. Ionic liquids for the convenient synthesis of functional nanoparticles and other inorganic nanostructures. *Angew. Chem. Int. Edit.* **43**, 4988–4992 (2004).
- 8 Ma, Z., Yu, J. H. & Dai, S. Preparation of Inorganic Materials Using Ionic Liquids. *Adv. Mater.* **22**, 261–285 (2010).
- 9 Torimoto, T., Tsuda, T., Okazaki, K. & Kuwabata, S. New frontiers in materials science opened by ionic liquids. *Adv. Mater.* **22**, 1196–1221 (2010).
- 10 Fukushima, T., Kosaka, A., Ishimura, Y., Yamamoto, T., Takigawa, N., Ishii, N. & Aida, T. Molecular ordering of organic molten salts triggered by single-walled carbon nanotubes. *Science* **300**, 2072–2074 (2003).
- 11 Ji, Q. M., Honma, I., Paek, S. M., Akada, M., Hill, J. P., Vinu, A. & Ariga, K. Layer-by-layer films of graphene and ionic liquids for highly selective gas sensing. *Angew. Chem. Int. Ed.* **49**, 9737–9739 (2010).
- 12 Hao, J. C. & Zemb, T. Self-assembled structures and chemical reactions in room-temperature ionic liquids. *Curr. Opin. Colloid Interface Sci.* **12**, 129–137 (2007).
- 13 Greaves, T. L. & Drummond, C. J. Ionic liquids as amphiphile self-assembly media. *Chem. Soc. Rev.* **37**, 1709–1726 (2008).
- 14 Nakashima, T., Zhu, J., Qin, M., Ho, S.-S. & Kotov, N. A. Polyelectrolyte and carbon nanotube multilayers made from ionic liquid solutions. *Nanoscale* **2**, 2084–2090 (2010).
- 15 Nakashima, T. & Kimizuka, N. Water/ionic liquid interfaces as fluid scaffolds for the two-dimensional self-assembly of charged nanospheres. *Langmuir* **27**, 1281–1285 (2011).
- 16 Kunitake, T. Synthetic bilayer-membranes—molecular design, self-organization, and application. *Angew. Chem. Int. Edit. Engl.* **31**, 709–726 (1992).
- 17 Ariga, K., Hill, J. P., Lee, M. V., Vinu, A., Charvet, R. & Acharya, S. Challenges and breakthroughs in recent research on self-assembly. *Sci. Technol. Adv. Mater.* **9**, 014109 (2008).
- 18 Kimizuka, N., Wakiyama, T., Miyauchi, H., Yoshimi, T., Tokuhito, M. & Kunitake, T. Formation of stable bilayer membranes in binary aqueous-organic media from a dialkyl amphiphile with a highly dipolar head group. *J. Am. Chem. Soc.* **118**, 5808–5809 (1996).

- 19 Kimizuka, N., Tokuhiro, M., Miyauchi, H., Wakiyama, T. & Kunitake, T. Bilayer formation in ethanol from dialkylammonium amphiphile appended with nitroaniline moiety. *Chem. Lett.* 1049–1050 (1997).
- 20 Ishikawa, Y., Kuwahara, H. & Kunitake, T. Self-assembly of bilayers from double-chain fluorocarbon amphiphiles in aprotic organic-solvents—thermodynamic origin and generalization of the bilayer assembly. *J. Am. Chem. Soc.* **116**, 5579–5591 (1994).
- 21 Kimizuka, N., Kawasaki, T., Hirata, K. & Kunitake, T. Tube-like nanostructures composed of networks of complementary hydrogen-bonds. *J. Am. Chem. Soc.* **117**, 6360–6361 (1995).
- 22 Kimizuka, N., Kawasaki, T., Hirata, K. & Kunitake, T. Supramolecular membranes. spontaneous assembly of aqueous bilayer membranes via formation of hydrogen bonded pairs of melamine and cyanuric acid derivatives. *J. Am. Chem. Soc.* **120**, 4094–4104 (1998).
- 23 Kimizuka, N. & Nakashima, T. Spontaneous self-assembly of glycolipid bilayer membranes in sugar-philic ionic liquids and formation of ionogels. *Langmuir* **17**, 6759–6761 (2001).
- 24 Nakashima, T. & Kimizuka, N. Vesicles in salt: formation of bilayer membranes from dialkyldimethylammonium bromides in ether-containing ionic liquids. *Chem. Lett.* 1018–1019 (2002).
- 25 Swatloski, R. P., Spear, S. K., Holvrey, J. D. & Rogers, R. D. Dissolution of cellulose with ionic liquids. *J. Am. Chem. Soc.* **124**, 4974 (2002).
- 26 Kunitake, T. & Okahata, Y. Totally synthetic bilayer membrane. *J. Am. Chem. Soc.* **99**, 3860–3861 (1977).
- 27 Ikeda, A., Sonoda, K., Ayabe, M., Tamaru, S., Nakashima, T., Kimizuka, N. & Shinkai, S. Gelation of ionic liquids with a low molecular-weight gelator showing T-gel above 100 °C. *Chem. Lett.* 1154–1155 (2001).
- 28 Hanabusa, K., Fukui, H., Suzuki, M. & Shirai, H. Specialist gelator for ionic liquids. *Langmuir* **21**, 10383–10390 (2005).
- 29 Tu, T., Bao, X. L., Assenmacher, W., Peterlik, H., Daniels, J. & Dotz, K. H. Efficient air-stable organometallic low-molecular-mass gelators for ionic liquids: synthesis, aggregation and application of pyridine-bridged bis(benzimidazolylidene)-palladium complexes. *Chem. Eur. J.* **15**, 1853–1861 (2009).
- 30 Dutta, S., Das, D., Dasgupta, A. & Das, P. K. Amino acid based low-molecular-weight ionogels as efficient dye-adsorbing agents and templates for the synthesis of TiO<sub>2</sub> nanoparticles. *Chem. Eur. J.* **16**, 1493–1505 (2010).
- 31 Yoshida, M., Kouimura, N., Misawa, Y., Tamaoki, N., Matsumoto, H., Kawanami, H., Kazaoui, S. & Minami, N. Oligomeric electrolyte as a multifunctional gelator. *J. Am. Chem. Soc.* **129**, 11039–11041 (2007).
- 32 Hao, J. C., Song, A., Wang, J., Chen, X., Zhuang, W., Shi, F., Zhou, F. & Liu, W. Self-assembled structure in room-temperature ionic liquids. *Chem. Eur. J.* **11**, 3936–3940 (2005).
- 33 Tang, J., Li, D., Sun, C.Y., Zheng, L.Z. & Li, J.H. Temperature dependant self-assembly of surfactant Brij 76 in room temperature ionic liquid. *Colloid Surf. A Physicochem. Eng. Asp.* **273**, 24–28 (2006).
- 34 He, Y. Y., Li, Z. B., Simone, P. & Lodge, T. P. Self-assembly of block copolymer micelles in an ionic liquid. *J. Am. Chem. Soc.* **128**, 2745–2750 (2006).
- 35 Lopes, J. & Padua, A. A. H. Nanostructural organization in ionic liquids. *J. Phys. Chem. B.* **110**, 3330–3335 (2006).
- 36 Fumino, K., Wulf, A. & Ludwig, R. Strong, localized, and directional hydrogen bonds fluidize ionic liquids. *Angew. Chem. Int. Edit.* **47**, 8731–8734 (2008).
- 37 Bonhote, P., Dias, A. P., Papageorgiou, N., Kalyanasundaram, K. & Grätzel, M. Hydrophobic, highly conductive ambient-temperature molten salts. *Inorg. Chem.* **35**, 1168–1178 (1996).
- 38 Nakashima, T. & Kimizuka, N. Light-harvesting supramolecular hydrogels assembled from short-legged cationic L-glutamate derivatives and anionic fluorophores. *Adv. Mater.* **14**, 1113–1116 (2002).
- 39 Kimizuka, N., Shimizu, M., Fujikawa, S., Fujimura, K., Sano, M. & Kunitake, T. AFM observation of organogel nanostructures on graphite in the gel-assisted transfer technique. *Chem. Lett.* 967–968 (1998).
- 40 Fei, Z. F., Ang, W. H., Zhao, D. B., Scopelliti, R., Zvereva, E. E., Katsyuba, S. A. & Dyson, P. J. Revisiting ether-derivatized imidazolium-based ionic liquids. *J. Phys. Chem. B.* **111**, 10095–10108 (2007).
- 41 Kimizuka, N., Takasaki, T. & Kunitake, T. Polymorphism in bilayer-membranes of novel double-chain ammonium amphiphiles. *Chem. Lett.* 1911–1914 (1988).

Supplementary Information accompanies the paper on Polymer Journal website (<http://www.nature.com/pj>)